

# Lifetime and fragment correlations for the two-neutron decay of $^{26}\text{O}$ ground state

L.V. Grigorenko,<sup>1,2,3</sup> I.G. Mukha,<sup>2</sup> and M.V. Zhukov<sup>4</sup>

<sup>1</sup>*Flerov Laboratory of Nuclear Reactions, JINR, Dubna, RU-141980 Russia*

<sup>2</sup>*GSI Helmholtzzentrum für Schwerionenforschung, Planckstraße 1, D-64291 Darmstadt, Germany*

<sup>3</sup>*National Research Center “Kurchatov Institute”, Kurchatov sq. 1, RU-123182 Moscow, Russia*

<sup>4</sup>*Fundamental Physics, Chalmers University of Technology, S-41296 Göteborg, Sweden*

The structure and decay of  $^{26}\text{O}$  are studied in a three-body  $^{24}\text{O}+n+n$  model. We have found extremely strong effect of the subbarrier configuration mixing on the width of true  $2n$  emitters due to core recoil and neutron-neutron final state interaction. This effect is far exceeding analogous effect in the true  $2p$  emitters. Our calculations provide reasonably narrow boundaries for the lifetime vs. decay energy dependence for the true  $2n$  emission. An upper limit of  $\sim 1$  keV for the decay energy of the unbound  $^{26}\text{O}$  is inferred basing on the recent experimental lifetime value.

PACS numbers: 21.60.Gx, 21.10.Tg, 21.45.+v, 23.90.+w

## I. INTRODUCTION

True few-body decay is an exclusive quantum mechanical phenomenon comprising simultaneous emission of several particles. Such a phenomenon leads to unusual lifetime systematics and complex correlation patterns for decay fragments. It takes place when the sequential emission of particles is prohibited by specific energy conditions. These conditions appear to be widespread beyond the nuclear driplines. Two-proton ( $2p$ ) radioactivity [1] and “democratic decay” [2] are the best-known specific examples of a broader true few-body decay phenomenon which were under scrutinous investigation in the last decade [3]. Nowadays, the studies of the neutron-rich systems beyond the proton dripline are very active. Recently there is an outburst of experimental results concerning the light true two-neutron ( $2n$ ) emitters:  $^{10}\text{He}$  [4–7],  $^{13}\text{Li}$  [8, 9],  $^{16}\text{Be}$  [10], and  $^{26}\text{O}$  [11–13].

The possibility of the very long-living (radioactive) neutron emitters was considered in the framework of simplified model in our work [14]. The true four-neutron emission was found to be the most prospective phenomenon for an experimental search. However, broad boundaries for existence of radioactive  $2n$  emitters were also estimated, naming the  $^{26}\text{O}$  system, information on which was absent at that moment, as one of the candidates. Since that time, upper limits were found experimentally for the decay energy of  $^{26}\text{O}$ :  $E_T = 150_{-150}^{+50}$  keV [11] and  $E_T < 120$  keV [12]. For known  $^{25}\text{O}$  ground state decay energy of  $770_{-10}^{+20}$  keV [17], the  $^{26}\text{O}$  is clearly ascribed to be a true  $2n$  emitter, see Fig. 1(a).

Recently the halflife of  $^{26}\text{O}$  was reported to be within the radioactivity timescale:  $T_{1/2} = 4.5_{-1.5}^{+1.1}(\text{stat}) \pm 3(\text{sys})$  ps [13]. Taking into account experimental complexities and novelty of the method the Authors express cautious optimism about possibility of two-neutron radioactivity observation in their work. Prospects of the discovery of this new type of the radioactive decay call for further focused experimental search and deeper theoretical insight, providing the guideline for such a search. This inspired us to perform more detailed studies of the long-living

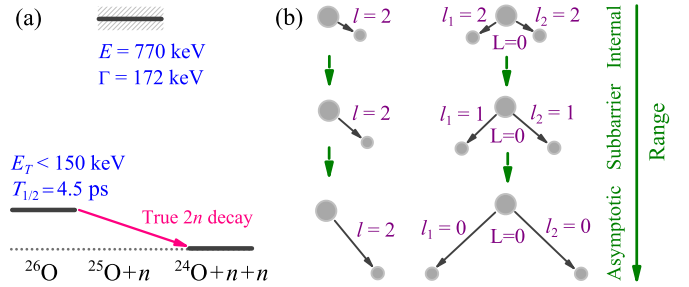


FIG. 1. (a) The energy scheme for  $2n$  decay of  $^{26}\text{O}$ . (b) Schematic comparison of two decay mechanisms: (i) in two-body decay the angular momentum  $l$  is conserved in the process of decay; (ii) in three-body decay of the  $[d^2]_{L=0}$  initial configuration, the subbarrier configuration mixing boosts the penetration drastically.

true  $2n$  emitters by example of the  $^{26}\text{O}$  system. Our work unveils complicated dynamical effects which should be accounted in calculations of true  $2n$  emitter’s widths. The important peculiarity of such a decay mechanism for  $^{26}\text{O}$  with  $[d^2]$  structure is schematically illustrated in Fig. 1(b).

## II. THEORETICAL MODEL

In studies of long-living true  $2n$  emitters we use the three-body hyperspherical harmonics (HH) cluster model developed for studies of  $2p$  radioactivity [15]. The model demonstrated applicability and high precision for broad range of decay energies, masses, and structures of  $2p$  precursors [3, 16]. In this approach the following sequence of problems is solved:

$$(\hat{H}_3 - E_T)\Psi_{\text{box}} = 0, \quad (1)$$

$$(\hat{H}_3 - E_T)\Psi^{(+)} = -i(\Gamma_{\text{arb}}/2)\Psi_{\text{box}}, \quad (2)$$

$$\Gamma = j/N, \quad (3)$$

where the eigenenergy  $E_T$  and corresponding eigenfunction  $\Psi_{\text{box}}$  are found as a solution of the homogenous

Schrödinger equation (1) with some “box” boundary conditions; next, the wave function (WF)  $\Psi^{(+)}$  with a pure outgoing three-body asymptotic is found by solving the inhomogeneous Schrödinger equation (2) with an arbitrary value of the width  $\Gamma_{\text{arb}}$ ; finally, the actual width  $\Gamma$  is defined in (3) via the outgoing flux  $j$  and internal normalization  $N$  connected with WF  $\Psi^{(+)}$ . The width values obtained in model calculations are shown in Figure 2.

### III. THREE-BODY CORRELATIONS

The three-body calculations in the HH method utilize the collective coordinates: the hyperradius  $\rho$  (describing collective radial motion) and the hyperangle  $\theta_\rho$  (responsible for geometry of the system at given  $\rho$ ):

$$\begin{aligned} \mathbf{x} &= \sqrt{\frac{A_1 A_2}{A_1 + A_2}} (\mathbf{r}_1 - \mathbf{r}_2), \\ \mathbf{y} &= \sqrt{\frac{(A_1 + A_2) A_3}{A_1 + A_2 + A_3}} \left( \frac{A_1 \mathbf{r}_1 + A_2 \mathbf{r}_2}{A_1 + A_2} - \mathbf{r}_3 \right), \\ \rho &= \sqrt{x^2 + y^2}, \quad \theta_\rho = \arctan(x/y). \end{aligned}$$

The boundary conditions of the HH method for the three-body decays without Coulomb interactions are well known. However, several effects, including the large scattering length in the  $n$ - $n$  channel, lead to slow radial and basis convergence of the calculations. The hyperradii up to 2000 fm are used depending on the decay energy. Some examples of the basis convergence are given in Figure 3.

In the momentum space the three-body energy-angular correlations (which actually can be measured, see [3]) are defined by the energy distribution parameter  $\varepsilon$  and the angle  $\theta_k$  between Jacobi momenta  $\mathbf{k}_x$  and  $\mathbf{k}_y$  (conjugated to Jacobi radii  $\mathbf{x}$  and  $\mathbf{y}$ ):

$$\begin{aligned} E_x &= \frac{A_1 + A_2}{2A_1 A_2 M} k_x^2, \quad E_y = \frac{A_1 + A_2 + A_3}{2(A_1 + A_2) A_3 M} k_y^2, \\ \varepsilon &= \frac{E_x}{E_x + E_y} = \frac{E_x}{E_T}, \quad \cos(\theta_k) = \frac{(\mathbf{k}_x, \mathbf{k}_y)}{k_x k_y}, \end{aligned}$$

where  $M$  is an average nucleon mass. For systems consisting of two nucleons and “core” these correlations could be defined in two Jacobi systems: “T” (particle 3 is the core) and “Y” (particle 3 is one of the nucleons). Coordinate and momentum space correlations for several cases of  $^{26}\text{O}$  calculations are given in Figure 4.

### IV. POTENTIALS

Taking into account the limited information on  $^{24}\text{O}$ - $n$  subsystem and exploratory character of our current studies, we use simplified potential sets. The  $n$ - $n$  potential, acting only in  $s$ -wave, is taken in the Gaussian form  $V(r) = -31 \exp[-(r/1.8)^2]$ . For the  $^{24}\text{O}$ - $n$  channel we

use a Woods-Saxon potential depending on the angular momentum ( $ls$  forces are not used). The only available data on  $^{25}\text{O}$  spectrum [17] allows to identify the ground state energy of  $770_{-10}^{+20}$  keV and the width of  $172 \pm 30$  keV which reliably indicates a  $d$ -wave state. Therefore, for the  $d$ -wave in the  $^{24}\text{O}$ - $n$  channel we use the potential with depth  $V_d = -35.5$  MeV, radius  $r_0 = 3.5$  fm, and diffuseness  $a = 0.75$  fm, which well reproduces the experimental properties of the resonance. The potential parameters for  $s$ - and  $p$ -waves used in different model calculations are given in Table I. The three-body potential depending on  $\rho$  with the typical Woods-Saxon parameterization [3] is used to control the decay energy  $E_T$  in the systematic lifetime calculations.

### V. CALCULATIONS WITHOUT $n$ - $n$ FINAL STATE INTERACTION (FSI)

The structure of  $^{26}\text{O}$  is expected to be dominated by the  $[d^2]$  configuration. If the decay proceeds also via the  $[d^2]$  configuration then the three-body model should provide the decay widths which have to be very close to the  $[d^2]$  estimate results from [14]. To reproduce formal conditions of this estimate in the three-body model, two actions are required: (i) the  $n$ - $n$  potential should be put to zero and (ii) the core mass should be infinite (actually the mass number  $\sim 100$  is a sufficient approximation). One can see in Fig. 2 that such three-body calculations (the solid curve) are very close to the generic  $[d^2]$  estimate, well following the energy trend  $\Gamma \sim E_T^6$  expected for the  $[d^2]_0$  decay.

The correlation patterns for this case are given in Fig. 4(a). One can see that the “triple-ridge” correlation connected with  $[d^2]_0$  coupling in the internal region survives to the asymptotics producing very symmetric “triple-peak” correlation in the energy distribution between neutrons in the Jacobi “T” system.

### VI. THE RECOIL EFFECT

The surprise comes when the core recoil is treated correctly with the right mass of the  $^{24}\text{O}$  fragment used in the “no FSI” calculations. The accounting for the recoil results in several orders of magnitude larger widths (the dashed curve in Fig. 2). The slope of the curve also evolves with the decay energy  $E_T$ . At the highest energy it is parallel to the  $[d^2]_0$  curve from [14]. With energy decrease it changes first to  $[p^2]$  then to  $s$ -wave slope at very small  $E_T$ . This indicates that the core recoil leads to configuration mixing allowing the WF to “migrate” into partial wave configurations with lower centrifugal barriers thus boosting the penetration, see Fig. 1(b).

Partial wave analysis and also the analysis of correlations confirm this idea. One can see in Fig. 4(b) that the triple-ridge  $[d^2]_0$  internal configuration is smearing out with radius increase and at about  $\rho = 150$  fm it is

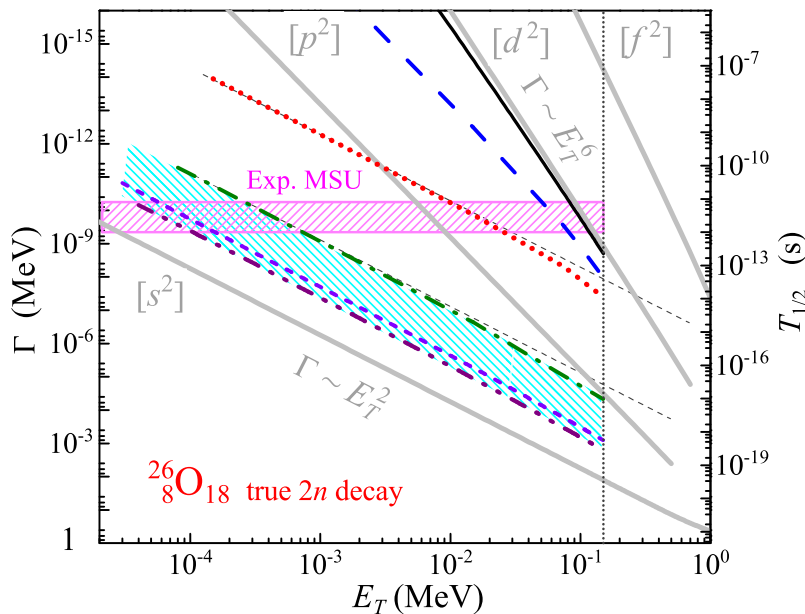


FIG. 2. (Color online) Width (half-life) of  $^{26}\text{O}$  as a function of its decay energy in different model calculations. Gray curves show the estimates of Ref. [14] for decay via pure orbital  $[l^2]$  configurations coupled to the total angular momentum  $L = 0$ . Solid curve shows the “no FSI, no recoil” case, dashed curve corresponds to “no FSI” situation. Dotted curve shows the results with  $n$ - $n$  FSI scaled by factor 0.25. Dash-dotted and dash-double-dotted curves correspond to “strong repulsion” and “moderate repulsion” in  $s$ - and  $p$ -waves in  $^{25}\text{O}$ , while short-dash curve shows the case with “no repulsion in  $p$ -wave”. Hatched areas give the experimental limits from Refs. [11, 13] and the realistic theoretical limits from this work.

replaced with a double-ridge configuration typical for a  $p$ -wave dominance. On asymptotics, this is reflected by a double-peak energy correlation between neutrons.

## VII. EFFECT OF THE $n$ - $n$ FSI

It is found to be much stronger in the case of true  $2n$  decay of  $^{26}\text{O}$  than it was typically observed in the case of

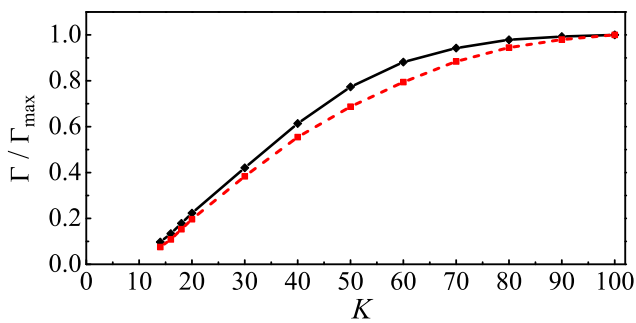


FIG. 3. Convergence of a width  $\Gamma$  as a function of generalized (hyperspherical) angular momentum  $K$ . Shown for the “moderate repulsion” case. Solid and dashed curves show calculations with  $E_T = 150$  and  $E_T = 1.5$  keV. For calculations above  $K = 20$  the hyperspherical channels are taken into account adiabatically.

the  $2p$  radioactivity (true  $2p$  decay). For illustration how this mechanism is engaged we performed the “1/4  $n$ - $n$  FSI” calculation with the  $n$ - $n$  potential multiplied by the 0.25 factor. Though giving only 4 times larger width than the “no FSI” calculation at  $E_T = 150$  keV, this model at smaller decay energies rapidly sticks to the  $[s^2]_0$  systematics providing dramatically larger widths. The triple-ridge correlation in the coordinate space pattern is now dissolved at much smaller radii [ $\rho \sim 80$  fm, see Fig. 4(c)], compared to the “no FSI” case. The energy correlation here shows one strongly asymmetric peak indicating the  $[s^2]/[p^2]$  configuration mixing, which is consistent with the trend of the  $[s^2]$  systematics.

The full  $n$ - $n$  FSI provides further drastic increase of the width (the dash-double-dotted curve in Fig. 2). The energy dependence is now completely following the  $[s^2]$  trend. The coordinate correlation patterns indicate very fast (just above  $\rho \sim 30$  fm) transition from the  $[d^2]$  to

TABLE I. Parameters of the Woods-Saxon potential in  $^{24}\text{O}$ - $n$  channel for different model cases. Radial parameters are in fm and  $V_i$  are in MeV.

Case	$V_s$	$V_p$	$r_0$	$a$
“1/4 $n$ - $n$ FSI”, “Moderate repulsion”	70	70	3.5	0.75
“no FSI”, “Strong repulsion”	120	120	5	1.2
“No repulsion in $p$ -wave”	70	0	3.5	0.75

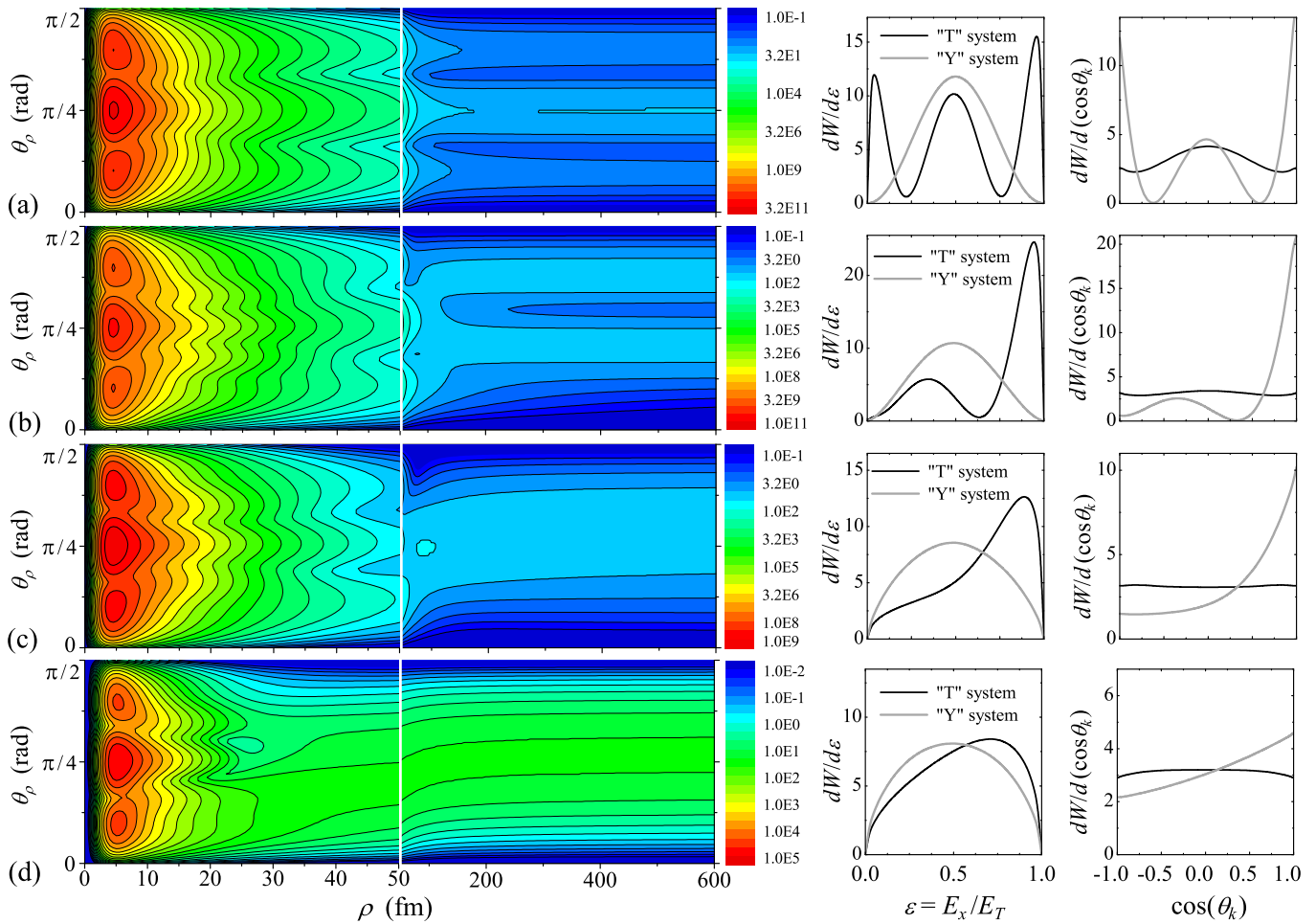


FIG. 4. (Color online) Correlations in  $^{26}\text{O}$  in different models: (a) “no FSI, no recoil”, (b) “no FSI”, (c) “1/4  $n$ - $n$  FSI” (d) “moderate repulsion”. Each row at two left panels shows the coordinate space correlation density for  $^{26}\text{O}$  WF  $\Psi^{(+)}$  on two different scales. Two right panels show the energy and angular (momentum space) correlations in “T” and “Y” Jacobi systems. All cases are calculated with  $E_T = 75$  keV.

the  $[s^2]$  configuration, see Fig. 4(d). The energy correlation between neutrons is now only slightly asymmetric indicating a dominance of the  $[s^2]$  configuration at the asymptotics already at  $E_T = 75$  keV.

### VIII. EFFECT OF THE OCCUPIED ORBITALS

In our model we use the repulsion in  $s$ - and  $p$ -waves as a simple method to account for the effect of the occupied orbitals in  $^{24}\text{O}$  in the absence of the experimental information about these interactions. To understand the importance of this aspect of the  $^{25}\text{O}$ - $n$  interaction for the  $^{26}\text{O}$  lifetime, we have performed calculations with very strong repulsive interactions in the  $s$ - and  $p$ -waves (the “strong repulsion” case) and without any nuclear interaction in the  $p$ -wave (the “no repulsion in  $p$ -wave” case). The widths in these calculations are different by a factor of 50 (see Fig. 2), while the lifetime energy systematics

and correlations patterns are not varying on a significant level. We may consider the band between the latter two cases as the realistic prediction range defined by the uncertainty of this aspect of our model. It should also be noted that the attractive  $s$ -wave interaction may further increase the provided widths. However, at the moment there is no evidence for such a possibility in the available experimental data.

### IX. DISCUSSION

Absence of Coulomb interaction in the case of long-living  $2n$  emitters, compared to the  $2p$  case, does not simplify, but makes the problem more complex in the sense of the sensitivity to several not well studied aspects of few-body dynamics. Nevertheless, we establish much narrower boundaries for the  $^{26}\text{O}$  lifetime thus providing the conservative upper limit of  $\sim 1$  keV for the decay

energy (assuming the lifetime from [13]).

If the experimental  $^{26}\text{O}$  lifetime is confirmed, the theoretically derived decay energy is very small on nuclear scale: the energy of  $^{26}\text{O}$  practically coincide with the  $2n$  threshold. This would mean extreme “halo like” structure of  $^{26}\text{O}$ . Formally, the radius of the decaying system is infinite. Practically, for systems with radioactive lifetimes the radial characteristics are reliably saturated for integration in the subbarrier region. We have found values around 5.5 fm for the “valence” neutron rms radius in  $^{26}\text{O}$ . Such values are typical for  $^{11}\text{Li}$  which possesses the most extreme  $2n$  halo known so far, which is connected mainly with the important  $[s^2]$  component of the WF. In  $^{26}\text{O}$  the analogous radial properties are expected despite the  $[d^2]$  component is dominating in the nuclear interior.

The expected from experimental lifetime and our calculations decay energy of less than 1 keV underlines the importance of special experimental techniques aimed at studies of such phenomena. The direct measurement of the  $^{26}\text{O}$  decay energy can provide an important cross check for possible discovery of the  $2n$  radioactivity in [13]. However, such small decay energies are not accessible for existing experimental setups: what we know so far is just the fact that  $^{26}\text{O}$  decays via  $2n$  emission with intractably small decay energy. A method, based on the precision measurements of neutron angular correlations in reactions with relativistic secondary beams, could overcome this problem. This method was proposed in Ref. [14] for future searches of  $2n$  and  $4n$  radioactivities and it is naturally suited for extreme low decay energies. Conceptually analogous method for decays with proton emission was found to be very robust [18].

## X. CONCLUSIONS

The detailed studies of possible long-living (radioactive) true  $2n$  emitters are performed for the first time by example of the  $^{26}\text{O}$  system. The following main results should be emphasized.

- (i) The fine few-body effects play extremely important role in the decay dynamics of the true  $2n$  emitters. The sensitivity of decay width to (a) configuration mixing due to core recoil, (b) subbarrier configuration mixing caused by  $n$ - $n$  FSI, and (c) occupied orbitals effects far exceeds the corresponding effects in true  $2p$  decays. Unexpectedly, the lifetime systematics of  $^{26}\text{O}$  with  $[d^2]$  internal structure sticks to the typical  $[s^2]$  behavior due to configuration mixing, see Fig. 1(b). Studies of the correlation patterns provide deep insights in the  $2n$  decay dynamics.
- (ii) The performed theoretical calculations provide much narrower limits for the lifetime vs. decay energy dependence of true  $2n$  decay of  $s$ - $d$  shell nuclei than those found in Ref. [14]. These narrower limits also provide much more stringent limits on the decay energies at which the  $2n$  radioactivity may be found.
- (iii) We discuss the recently observed evidence for a  $2n$  radioactivity of  $^{26}\text{O}$  (its lifetime is reported to be in a picosecond range). Being confirmed such a lifetime means extremely low decay energy of  $^{26}\text{O}$  (below  $\sim 1$  keV) and calls for special experimental techniques for further studies of this phenomenon.

*Acknowledgments.* — L.V.G. is supported by the Helmholtz Association under grant agreement IK-RU-002 via FAIR-Russia Research Center and by Russian Foundation for Basic Research 11-02-00657-a and Ministry of Education and Science NS-215.2012.2 grants.

- 
- [1] V.I. Goldansky, Nucl. Phys. **19**, 482 (1960).
  - [2] O.V. Bochkarev *et al.*, Nucl. Phys. **A505** 215, (1989).
  - [3] M. Pfützner, L.V. Grigorenko, M. Karny, K. Riisager Rev. Mod. Phys. **84**, 567 (2012).
  - [4] M.S. Golovkov *et al.*, Phys. Lett. B **672**, 22 (2009).
  - [5] H.T. Johansson *et al.*, Nucl. Phys. **A842**, 15 (2010).
  - [6] S.I. Sidorchuk *et al.*, Phys. Rev. Lett. **108**, 202502 (2012).
  - [7] Z. Kohley *et al.*, Phys. Rev. Lett. **109**, 232501 (2012).
  - [8] Yu. Aksyutina *et al.*, Phys. Lett. B **666**, 430 (2008).
  - [9] Z. Kohley *et al.*, Phys. Rev. C **87**, 011304(R) (2013).
  - [10] A. Spyrou *et al.*, Phys. Rev. Lett. **108**, 102501 (2012).
  - [11] E. Lunderberg *et al.*, Phys. Rev. Lett. **108**, 142503 (2012).
  - [12] C. Caesar *et al.*, arXiv:1209.0156.
  - [13] Z. Kohley *et al.*, Phys. Rev. Lett. **110**, 152501 (2013).
  - [14] L.V. Grigorenko, I.G. Mukha, C. Scheidenberger, M.V. Zhukov, Phys. Rev. C **84**, 021303(R) (2011).
  - [15] L.V. Grigorenko, R.C. Johnson, I.G. Mukha, I.J. Thompson, and M.V. Zhukov, Phys. Rev. Lett. **85**, 22 (2000).
  - [16] I.A. Egorova *et al.*, Phys. Rev. Lett. **109**, 202502 (2012).
  - [17] C.R. Hoffman *et al.*, Phys. Rev. Lett. **100**, 152502 (2008).
  - [18] I. Mukha *et al.*, Phys. Rev. Lett. **99**, 182501 (2007).